Chemical Tuning of Metal-Semiconductor Interfaces

D. A. Ricci,[1,2] T. Miller,[1,2] and T.-C. Chiang[1,2]

[1]*Department of Physics, University of Illinois at Urbana-Champaign, 1110 West Green Street, Urbana, Illinois 61801-3080, USA*
[2]*Frederick Seitz Materials Research Laboratory, University of Illinois at Urbana-Champaign, 104 South Goodwin Avenue,
Urbana, Illinois 61801-2902, USA*

We report a study of the Schottky barrier for Pb films grown on Si surfaces terminated by various metals (Ag, In, Au, and Pb) to explore the atomic-scale physics of the interface barrier and a means to control the barrier height. Electronic confinement by the Schottky barrier results in quantum well states in the Pb films, which are measured by angle-resolved photoemission. The barrier height is determined from the atomic-layer-resolved energy levels and the line widths. A calculation based on the known interface chemistry and the electronegativity yields predicted barrier heights in good agreement with the experiment.

PACS numbers: 73.21.Fg, 73.30.+y

The Schottky barrier is an important feature of solid-state electronic devices involving metal films on semiconductor substrates [1–19]. It determines the rectifying and transport properties of the interface and the quantum well electronic structure of the film. These characteristics of the Schottky barrier are critical for solid-state device design, particularly as the field is evolving toward a length scale in which quantum effects dominate. Atomic-level control and accurate determination of the barrier height have been long-standing issues [1–19]. This work is a study of Pb films grown on several metal-terminated Si(111) surfaces to illustrate the systematics and strategies toward a solution. The metals used for termination include Ag, In, Au, and Pb, and the resulting barrier heights are significantly different among the four systems. An analysis of the results establishes that the electronegativity of the metal used for Si termination determines a charge transfer at the interface, which in turn gives rise to an interface dipole layer that determines the barrier height. Schottky barrier heights are predicted based on the standard Mulliken electronegativity table, with no adjustable parameters, and the results are in excellent agreement with the measurements. The findings offer an important insight into the basic atomic-level physics of the Schottky barrier that is important for barrier engineering.

Angle-resolved photoemission is employed to determine the barrier height in each case. Quantum confinement by the Schottky barrier results in quantum well states in the film [20–22]. The energies of these states are measured for a number of film thicknesses, from which the barrier height is deduced. The results are complemented and confirmed by a measurement of the quantum well peak widths. States in the quantum well fully confined by the barrier have narrow line shapes, while resonance states with energies outside the barrier are much broader due to degenerate coupling of the electronic states. A substantial change in line width indicates the location of the confinement edge and the barrier height. For both the energy and line width measurements, it is essential that the absolute film thickness be controlled with monolayer precision. All systems chosen for this study meet this requirement. Furthermore, the Pb films in all cases have the same epitaxial relationship and structure; thus, the resulting differences can be unequivocally attributed to interfacial effects. Previous Schottky barrier measurements mostly relied on core level spectroscopy, but the method is generally limited to few atomic layers for which the interface and the overlayer are not necessarily fully developed. It is thus difficult to separate out effects pertaining to the surface, the adsorbate, and the interface. Photovoltaic effects have also been shown to obscure the accurate measurement of barrier heights in core level studies of ultrathin films [19]. Diode measurements are free from such uncertainties, but sample fabrication with atomically controlled interfaces is extremely difficult, and existing data are scarce [9,10].

Three metal-terminated Si(111) surfaces were created on n-type Si(111) by molecular beam epitaxy, including the Ag-$\sqrt{3} \times \sqrt{3}$, In-$\sqrt{3} \times \sqrt{3}$, and Au-6×6 reconstructed surfaces, with the metal coverages of 0.33, 0.33, and 0.96 monolayers (ML), respectively, in substrate units (1 ML = 7.83×10^{14} atoms/cm^2) [23–25]. The Si(111) substrates were cut from commercial n-doped wafers with a resistivity of 1-60 Ω − cm and were thermally cleaned by resistive heating *in vacuo* to remove the surface oxide layer and to produce the 7×7 surface upon which the metal reconstructions were formed. All molecular beam epitaxy was performed via evaporation from e-beam-heated crucibles. Reconstructions with well-defined periodicities were chosen as the interfactant layers because they provide the ordered surface necessary to grow smooth films that can support quantum well states [26,27].

Thin Pb films were grown over the substrates at 100 K. For all Pb film thicknesses, one ML is defined in terms of

bulk Pb (9.43×10^{14} atoms/cm^2). The resulting films were oriented along the (111) direction. The photoemission measurements were performed on undulator beamlines at the Synchrotron Radiation Center, University of Wisconsin-Madison, using 22 eV photons, with the sample at 100 K. Photoemission data were acquired with either a Scienta SES100 or a EA125 hemispherical analyzer mounted on an ultrahigh vacuum chamber with a base pressure of 8×10^{-11} torr. Quantum well data for Pb films grown on the Pb-$\sqrt{3} \times \sqrt{3}$ terminated Si(111) surface (coverage 0.33 ML) were adapted from previous work [28].

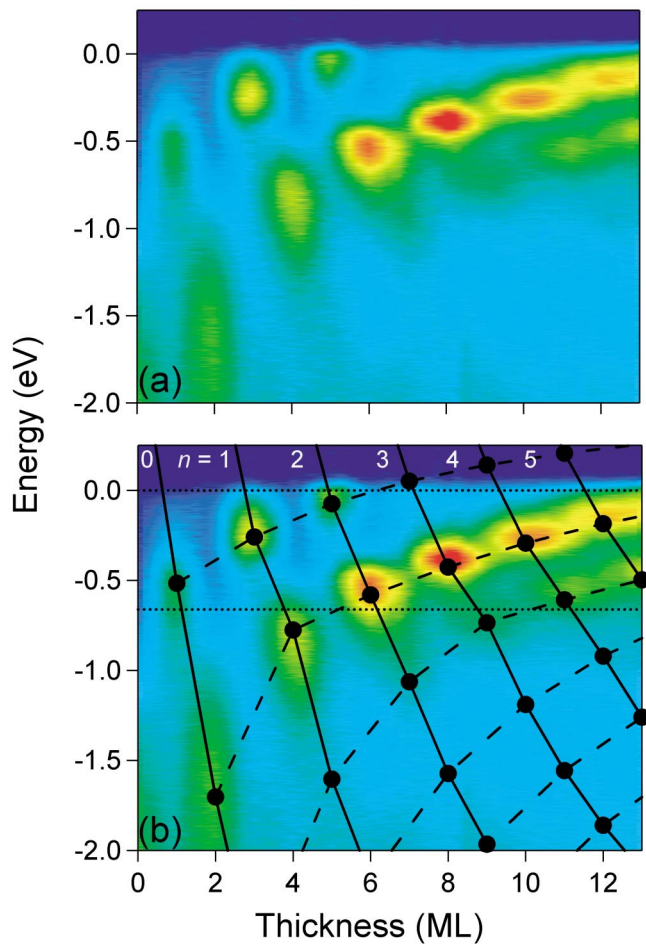The gray-scale image in Fig. 1 shows the normal-emission intensity as a function of energy and Pb film

FIG. 1 (color online). (A) Photoemission intensity as a function of energy and film thickness for Pb films deposited on the Au-6 × 6 terminated Si(111) surface. The intensity maxima (brighter regions) correspond to quantum well states. (B) The solid curves indicated the evolution of the quantum well energies based on a simultaneous fit to the data for the four systems. The quantum number n for each branch is indicated. The dashed lines indicate the branches based on the alternate quantum number $p = N - 2n - 1$ used previously for rough films.

thickness for the Au-6 × 6 terminated Si(111) surface for coverages from 0 to 13 ML. The most notable features are the discrete peaks that represent the confinement of Pb valence electrons between the vacuum and the Si band gap. These peaks are fully developed at integer monolayer film thicknesses, and the atomic-layer resolution permits a determination of the absolute film thickness by atomic-layer counting [29]. The less intense, broader peaks at higher binding energies are the quantum well resonances derived from partially confined electrons. The results for the other three metal-terminated Si surfaces are similar and not shown. The energy levels at a given thickness for the different systems can vary by up to ~0.6 eV. The quantum well energy levels are determined by the Bohr-Sommerfeld quantization rule [20–22]:

$$2k(E)Nt + \phi_v + \phi_s = 2n\pi \qquad (1)$$

where k is the electron momentum, E is the energy of the state, N is the number of Pb monolayers, t is the monolayer thickness, ϕ_v and ϕ_s are the energy-dependent phase shifts at the vacuum and substrate interfaces, respectively, and n is a quantum number. The substrate phase shift ϕ_s has a singularity at the valence band maximum of Si at E_0 and is given, to the leading order, by

$$\phi_s(E) = A + B\sqrt{E - E_0}\Theta(E - E_0), \qquad (2)$$

where A and B are constants [30]. The bulk band dispersion $k(E)$ and the vacuum phase shift $\phi_v(E)$ are known from a first-principles calculation [31]. Eqs. (1) and (2) are used to fit the observed quantum well energy levels for all four systems simultaneously. The quantity B is tied to the Si band edge, and should be the same for all four systems. The quantity A depends on the atomic details of the interface, and is allowed to vary among the systems. The quantity E_0, the confinement energy relative to the Fermi edge, also depends on the system. The Si gap, 1.15 eV, subtracted by E_0, equals the Schottky barrier height for the n-type substrates[8]. No other fitting parameters are involved. The results of the fit are shown as the solid curves in Fig. 1 for the Au-6 × 6 system, and the quantum number n for each branch is indicated. The dashed lines represent branches based on the alternate quantum number $p = N - 2n - 1$ in use in the literature [32]. In earlier studies, the films had a significant roughness, causing the peaks as seen in Fig. 1 to smear out to form continuous bands following the dashed lines.

An independent determination of the Schottky barrier heights is provided by a measurement of the quantum well peak widths as explained above. The results are shown in Fig. 2, where the circles represent the measured widths for various thicknesses and quantum numbers for the four systems. In each case, the measured width exhibits a threshold in energy below which it increases rapidly. The vertical lines indicate the midpoint locations bracketed by a sudden change in peak width, and these

are seen to well represent the threshold positions. The Schottky barrier heights S_{expt} synthesized as weighted averages from these measurements and the results of the preceding fit are given in Table I (last column).

Table I contains the Mulliken electronegativity χ and the coverage C for the metals at the interface for the four terminations studied (Ag, In, Au, and Pb) as well as for three other hypothetical cases (Fr, Si, and F) for reference purposes, organized in ascending orders of the electronegativity. The two elements Fr and F represent the two extreme cases on the electronegativity scale of the periodic table. The quantity Q is the average charge state of the Si in direct contact with the interfacial metal (M) layer. It is deduced by first evaluating the coverage-weighted electronegativity for the interfacial metal layer (which may be partly Pb), subtracting the electronegativity of Si, and then normalizing the results to one half of the electronegativity difference between F and Fr. Thus,

$$Q = \frac{[C\chi_M + (1 - C)\chi_{Pb}] - \chi_{Si}}{(\chi_F - \chi_{Fr})/2}. \tag{3}$$
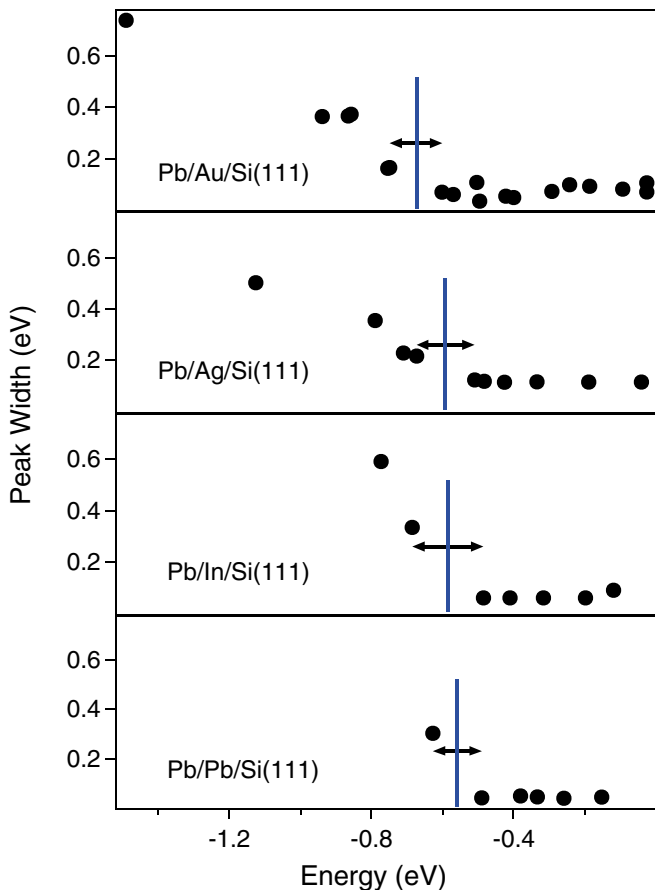

FIG. 2 (color online). Width of quantum well peaks as a function of energy for the four terminations studied. The vertical line in each case denotes the position of the confinement edge as the midpoint between the adjacent confined and resonant peak widths.

For the hypothetical case of F termination, the numerical result is $Q = 1$. This is the most electronegative element in the periodic table, and the Si in direct contact with F is in the +1 oxidation state. Likewise, $Q = -1$ for Fr, the most electropositive element. For Si termination, $Q = 0$ as expected, meaning that the charge state remains neutral. Also included in Table I are the calculated Schottky barrier heights based on a linear mapping from the Q scale:

$$S_{\text{cal}} = \frac{Q + 1}{2} E_g, \tag{4}$$

where 1.15 eV is the Si gap at 100 K. The mapping is linear because the charge state Q is proportional to the interface dipole, which contributes directly to the barrier height. The coefficients of the mapping are verified as follows. Considering F termination, the Si layer in direct contact is in the +1 charge state (but not the next layer). This means that the Fermi level at the interface must be pinned at the conduction band edge, resulting in an ionized interface Si layer. For the n-type substrates used in this experiment, $S = E_g$, and this is exactly what Eq. (4) yields. Likewise, for Fr termination, where the Si layer at the interface is in a -1 charge state, $S = 0$ based on similar physical arguments, and this is also what Eq. (4) yields.

The calculated Schottky barriers from Eq. (4) for the four systems are included in Table I for comparison. The results are also shown in Fig. 3 where the measured Schottky barrier heights (dots) are compared with the calculated barrier heights (line) as a function of the interfacial Si charge state Q. The agreement is very good in that the calculation reproduces the overall trend and its correlation with Q. This level of quantitative agreement is remarkable considering the simplicity of the model which involves only the known chemical composition of the interface and the well established electronegativity table.

To recap, the "surface sensitive" technique of valence band photoemission has been used in a novel manner to

TABLE I. Electronegativity (χ), interface coverage (C), interface Si charge state (Q), and the calculated and experimental Schottky barrier height (S_{calc} and S_{expt}) for the four metals used for Si termination (Ag, In, Au, and Pb) and for three other relevant hypothetical cases (Fr, Si, and F).

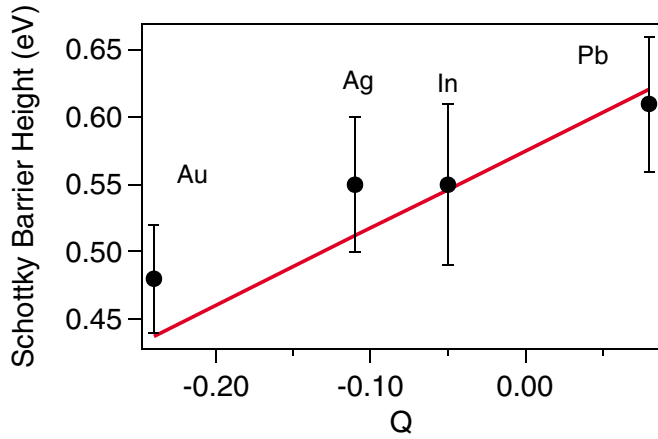|	χ	C	Q	S_{cal}(eV)	S_{expt}(eV)
Fr	0.68	1	-1	0	
Ag	1.47	0.33	-0.11	0.51	0.55 ± 0.05
In	1.76	0.33	-0.05	0.55	0.55 ± 0.06
Au	1.87	0.96	-0.24	0.44	0.48 ± 0.04
Si	2.28	1	0	0.58	
Pb	2.41	1	0.08	0.62	0.61 ± 0.05
F	3.91	1	1	1.15	

FIG. 3 (color online). Experimental (circles) and predicted (line) Schottky barrier heights plotted against the interface Si charge parameter Q.

probe the Schottky barrier by exploiting the interface dependence of quantum wells. This study shows that metal termination of Si surfaces prior to film deposition can be an effective means for Schottky barrier engineering. The electronegativity of the metal, together with the coverage, determines a net charge transfer. The resulting interface dipole layer gives rise to a potential difference directly contributing to the barrier. An important insight derived from the present study is that the charge state of the interfacial Si can be directly tied to the barrier height, without any assumptions about the thickness of the dipole layer and the effective dielectric constant at the interface as have been discussed extensively in the literature [1–3]. This insight and the predictive power of the model are of value to barrier engineering at the atomic level.

[1] R. T. Tung, Mater. Sci. Eng., R **35**, 1 (2001).
[2] R. T. Tung, Phys. Rev. Lett. **84**, 6078 (2000).
[3] D. Cahen and A. Kahn, Adv. Mater. **15**, 271 (2003).
[4] R. A. McKee, F. J. Walker, M. B. Nardelli, W. A. Shelton, and G. M. Stocks, Science **300**, 1726 (2003).
[5] A. Vilan, A. Shanzer, and D. Cahen, Nature (London) **404**, 166 (2000).
[6] H. Hirayama, T. Yamaguchi, H. Ikezawa, and K. Tanaka, Phys. Rev. B **66**, 073301 (2002).
[7] K. Horn, Appl. Surf. Sci. **166**, 1 (2000).
[8] L. Aballe, C. Rogero, P. Kratzer, S. Gokhale, and K. Horn, Phys. Rev. Lett. **87**, 156801 (2001).
[9] R. F. Schmitsdorf and W. Mönch, Eur. Phys. J. B **7**, 457 (1999).
[10] D. R. Heslinga, H. H. Weitering, D. P. van der Werf, T. M. Klapwijk, and T. Hibma, Phys. Rev. Lett. **64**, 1589 (1990).
[11] L. J. Brillson, Surf. Sci. **299/300**, 909 (1994).
[12] G. Margaritondo, Rep. Prog. Phys. **62**, 765 (1999).
[13] J. H. Weaver, in *Electronic Materials: A New Era of Materials Science*, Springer Ser. Solid-State Sci. Vol. 95 (Spring-Verlag, Berlin, 1991), Chap. 8, p. 135−214.
[14] I. Lindau, T. Kendelewicz, N. Newman, R. S. List, M. D. Williams, and W. E. Spicer, Surf. Sci. **162**, 591 (1985).
[15] G. W. Rubloff, in *Dynamical Phenomena at Surfaces, Interfaces and Superlattices. Proceedings of an International Summer School* (Springer-Verlag, Berlin, 1985), Vol. 1-13, p. 220−243.
[16] J. L. Freeouf, Surf. Sci. **132**, 233 (1983).
[17] R. Ludeke, Surf. Sci. **132**, 143 (1983).
[18] W. E. Spicer, R. Cao, K. Miyano, T. Kendelewicz, I. Lindau, E. Weber, Z. Liliental-Weber, and N. Newman, Appl. Surf. Sci. **41-42**, 1 (1989).
[19] M. H. Hecht, Phys. Rev. B **41**, 7918 (1990).
[20] T.-C. Chiang, Surf. Sci. Rep. **39**, 181 (2000).
[21] S.-A. Lindgren and L. Wallden, *Electronic Structure*, Handbook of Surface Science Vol. 2 (Elsevier, New York, 2000).
[22] M. Milun, P. Pervan, and D. P. Woodruff, Rep. Prog. Phys. **65**, 99 (2002).
[23] L. S. O. Johansson, E. Landemark, C. J. Karlsson, and R. I. G. Uhrberg, Phys. Rev. Lett. **63**, 2092 (1989).
[24] S. Mizuno, Y. O. Mizuno, and H. Tochihara, Phys. Rev. B **67**, 195410 (2003).
[25] T. Nagao, S. Hasegawa, K. Tsuchie, S. Ino, C. Voges, G. Klos, H. Pfnur, and M. Henzler, Phys. Rev. B **57**, 10100 (1998).
[26] M. Jalochowski, H. Knoppe, G. Lilienkamp, and E. Bauer, Phys. Rev. B **46**, 4693 (1992).
[27] T. Schmidt and E. Bauer, Phys. Rev. B **62**, 15815 (2000).
[28] M. H. Upton, C. M. Wei, M. Y. Chou, T. Miller, and T.-C. Chiang, Phys. Rev. Lett. **93**, 026802 (2004).
[29] J. J. Paggel, T. Miller, and T.-C. Chiang, Phys. Rev. Lett. **81**, 5632 (1998).
[30] M. A. Mueller, A. Samsavar, T. Miller, and T.-C. Chiang, Phys. Rev. B **40**, 5845 (1989).
[31] C. M. Wei and M. Y. Chou, Phys. Rev. B **66**, 233408 (2002).
[32] A. Mans, J. H. Dil, A. R. H. F. Ettema, and H. H. Weitering, Phys. Rev. B **66**, 195410 (2002).